
Journal of Engineering Technology and Applied Physics

Automated Measurement of Stone Heterogeneity Index and Variation Coefficient of Stone Density on CT Image

Lai Yee Myint^{1,*} and Khine Thin Zar²

¹Department of Information Technology Engineering, West Yangon Technological University, Yangon, Myanmar.

²Department of Computer Engineering and Information Technology, Yangon Technological University, Yangon, Myanmar.

*Corresponding author: khinetz2021@gmail.com, ORCID: 0009-0000-1482-4471

<https://doi.org/10.33093/jetap.2023.5.1.6>

Manuscript Received: 16 February 2023, Accepted: 13 March 2023, Published: 15 March 2023

Abstract — Heterogeneity is a key feature of stone density as Hounsfield Unit (HU) on computer tomography (CT) for extracorporeal shock-wave lithotripsy (ESWL) outcomes predicting in urinary calculi patients. The goal of this study is to develop the modified 2D and 3D automate stone heterogeneity index and variation coefficient of stone density estimation program to predict ESWL treatment. For 2D, the proposed program was selected the largest slice of the stone in the whole input slice and then stone related variables, stone heterogeneity index and variation coefficient of stone density were calculated by using the average HU and the number of voxels of the stone. For these variables, it was also developed 3D automate system by using all slices including the stone. Moreover, the 2D schematic diagram was produced to show the internal structure of stone in order to estimate the compositional heterogeneity of stone. All processes of this study were established without manual process. And then, the result of the proposed study is presented compared with the manual measurements. The described methods can provide to assist the prediction of ESWL treatment success and urinary stone diagnosis.

Keywords—Stone heterogeneity index, Variation Coefficient of stone density, Internal structure of stone, ESWL treatment, Hounsfield Units (HU)

I. INTRODUCTION

Although there are the widespread acceptance and the high success rate of ESWL, it was still partially or completely resistant for urinary calculi [1]. Moreover, the first ESWL failure may be some problem such the continuation of symptoms and ureteral obstruction that increase medical costs because of the ancillary therapy procedures requirement. Therefore, the ESWL

outcome prediction factors and a suitable treatment selection are essential and effective for patients with urinary calculi [2]. Nowadays, computer tomography (CT), an excellent non-invasive imaging, is a highly recommended examination for urinary stone treatment planning. It is used for assessing several predictive factors. These useful parameters were included stone location, stone size (area, volume, diameter), mean stone density (average HU), stone heterogeneity index (standard deviation), and variation coefficient of stone density. The increasing number of studies were reported the usefulness of these several factors that manually and semi-automatically measured on CT images [5 - 7]. Most of previous studies have focused on the HU value [3], stone size [4] and location [5] to assist stone diagnosis and treatment planning. There are still inadequate CT parameters predictions for clinical use. In addition, stone density, other parameter about stone heterogeneity is also analysis in CT parameter prediction.

And then, understanding three-dimensional visualization of urinary stone is crucial for planning and creating an optimal access route. So, 3D visualization of CT data and internal composition are increasing with the use of advanced imaging [8, 9]. Advanced imaging systems have been provided to access the 3D visualization of target object and internal structure of this object. Especially, 3D visualization is useful to provide the shape of object and internal structure of object is also vital to provide the composition inside of object. This is a continuous search for new and improved methods that could assist at urinary stone treatment planning. For the purpose of

this study, the automate measurement of stone heterogeneity index and variation coefficient of stone density were created with 3D visualization and 2D internal structure of stones.

II. PREVIOUS STUDIES

In [1], this study was also investigated the standard deviation of HU on CT as stone heterogeneity index (SHI) in order to predict ESWL outcomes for ureteral stones patients. It was analysis two groups, low SHI and high SHI groups that categorized by using mean SHI. The low SHI group was not as better as the high SHI group in one-session success rate. It reported that SHI values were useful as an independent predictor for ESWL success in urinary calculi patients and an effective parameter for the fragility of stone.

In [2], they reported the important of SHI and variation coefficient of stone density (VCSD) to identify WSWL outcome and choose the appropriate treatment decision for urinary calculi patients. In here, SHI value was manually measured the standard deviation from the information of CT images. VCSD was calculated this SHI value divided by the average value. It could define that SHI and VCSD were effective and efficient as an independent significant predictor for ESWL success in urinary calculi.

In [6], heterogeneity in CT image was measured to develop an octree decomposition and variogram analysis which provide a non-objective and sensitive metric. This metric could characterize emphysematous lung disease. Although the system semi-automatically developed a mask image using ImageJ and ImageJ 3D Toolkit plug-in, a novel and objective method was presented to assess lung damage in CT. In here, heterogeneity index was measured and used to present the difference of an individual variogram and the control average. It could show the clear separation in characterizing lung disease such as control, mild global disease and severe local disease.

In [10], it was to assess the important of stone heterogeneity index, a helping tool for SWL success rates. SHI was manually described by computing the HU standard deviation in the specified region. In this study, SHI was clearly distinguished between stone free and stone failure EWSL rate for patients having average HU 500 _ 1000 values. It indicated that SHI can be effective to assess the extent of fragility of the stone.

In previous study, stone features on CT were described as stone attributes such as stone size, location, average HU. Later, SHI and VCSD were designated to estimate the heterogeneity of the stone. It was assumed that heterogeneous stone was more fragile than homogeneous one. In this study, it was adopted the modified concept without manual process into stone heterogeneity index and variation coefficient stone density for 2D and 3D CT measurements. Moreover, 2D internal structure of the

stone was displayed to estimate the composition of the urinary calculi.

III. PROPOSED METHODOLOGY

The proposed system is presented in this paper in order to develop three CT parameters from urinary calculi CT images. In CT imaging, these CT parameters cannot be neglected to assist for diagnosis of urinary calculi patients.

In this paper, we developed both 2D and 3D CT parameters measurements, automatically. The overall process flow of the proposed approach is presented in Fig. 1. First, the preprocessing is a step to segment the stone region by removing other unwanted region removing in the image that used both for 2D and 3D auto measurements. But there was an additional process, largest slice selection among all slices of the stone in 2D Auto measurements. In 2D process, it was provided an assessment of average HU and standard deviation only on this selected slice and then calculated the variation coefficient of stone density (VCSD) by using these two parameters.

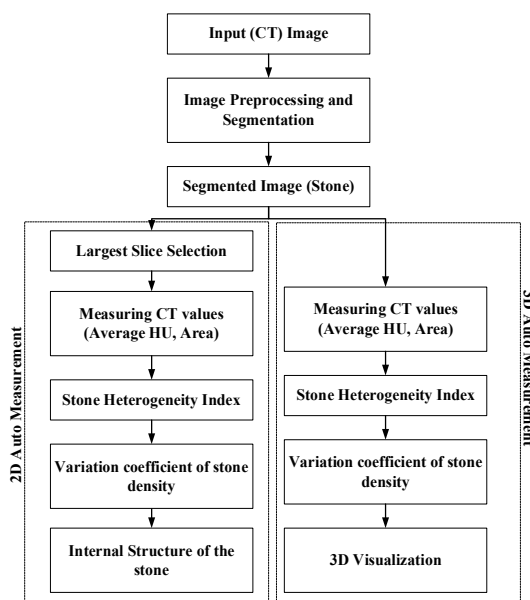


Fig. 1. The flow diagram of the proposed 2D and 3D measurements.

Next, stone composition is also presented with HU value of each pixel in internal structure of stone. It assists to estimate that heterogeneity or homogeneity of stone.

Because of no volumetric information, there are some limitations in 2D measurements such as stone number, length and shape. It may be significant for larger, irregularly shaped stones. The increase size of stones, more random the shape of stone becomes. So, it is essential 3D object by using 3D reconstructing to provide the volumetric information [4]. Therefore, 3D visualization and parameters as measured by 3D reconstruction object are becomes a powerful approach to increase the understanding of medical CT images and clinical support. In this study, 3D auto measurement was developed without largest slice

selection. Unlike 2D process, it was to treat 3D parameters predictions in a series of 2D image slices including the stone region. Using all these slices, average HU, standard deviation and VCSD are extracted with the same method of 2D process. Moreover, it can present the clear 3D urinary stone object with rotation options. To reduce the inaccuracy of the manual measuring, the following steps are applied in the proposed algorithm, which is briefly described in this section.

A. Image Pre-processing and Segmentation

In abdominal CT image, there are many unwanted regions and organs surrounding urinary calculi. It is needed to distinguish the calculi with these unwanted objects in order to measure the CT parameters for the urinary calculi. Therefore, the pre-processing process is essential to be done. Figure 2 shows pre-processing of urinary calculi segmentation by removing other unwanted objects, which consists of the following steps:

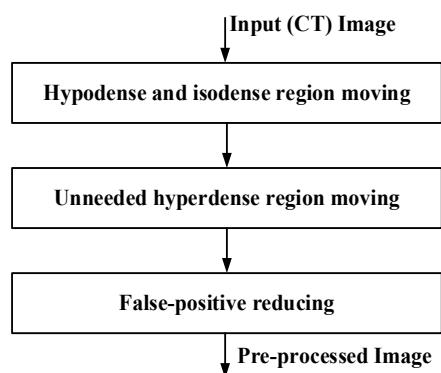


Fig. 2. The flow diagram of the pre-processing.

In above three processes, thresholding is the vital method to remove the unwanted regions. The require threshold value of each process is calculated based on the nature of the urinary calculi and other surrounding objects of the CT. In first process, threshold value is calculated based on the intensity differences between the urinary calculi (bright-white high intensity) and another region (Gray to black low intensity) on CT. Intensity of stone could be a range between 200 HU and 2800 HU, which are used as threshold value of hypodense and isodense region removal.

In second process, hyperdense regions similar with stone intensity were removed using size-based thresholding. The size of stone was regarded between 3 mm and 50 mm which range used as threshold value.

In final process of pre-processing, the modified thresholding was used to reduce false-positive by applying average HU and volume ratio. It was regarded this modified threshold value as a range between 0.03 and 35. The unwanted regions were removed from the image using these three pre-processing processes and then it was produced the segmented regions (urinary calculi) which were used to measure the required CT parameters.

B. Largest Slice Selection

Using binarization, the segmented region of the image is converted into a binary image. This binary image and the whole image including HU values were combined with a logical "AND" operation to take the foreground pixels with HU value in the image. According to the help of "AND" operation and binarization, it was taken the foreground pixels with HU values as the stone region. After that, it was calculated the sum of all foreground pixels and then the number of pixels of each slice were compared in order to take the largest slice of the stone. According these processes, it can take only HU values of pixels in stone region at the largest slice of the stone. These values were used to measure and calculate the required CT parameters of the proposed system.

C. Measuring CT Values

In the proposed study, CT values are measured by taking all HU value for each pixel on the segmented region of the largest slice of the whole stone. To calculate the required Stone Heterogeneity Index and Variation coefficient of stone density, there are two essential CT values average Hounsfield units and area of the segmented region.

Average Hounsfield Units (Average HU) is calculated by adding HU values of all pixels in the segmented region and then dividing the count of those pixels. Area is the total number of pixels in the selected region.

D. Stone Heterogeneity Index

One of CT parameters, stone heterogeneity, is important to consider the internal structure of stone in CT. Standard deviation of HU on CT is used to define the stone heterogeneity. Higher standard deviation of HUs on CT be, more heterogeneity of internal structure on stone be [1]. Therefore, standard deviation is calculated to define the stone heterogeneity in this study.

$$SD = \sqrt{\frac{\sum(x_i - x_{mean})^2}{N-1}} \quad (1)$$

, where SD means standard deviation, x_i and x_{mean} are individual pixel value and average of all pixel values in the segmented region, and N is the total number of pixels in this region.

E. Variation Coefficient of Stone Density (VCSD)

Sometime, there may be differ in the stone composition even if the stones have a similar mean or SD. Therefore, variation coefficient of stone density becomes another consideration with stone heterogeneity [7]. VCSD is the ratio of standard deviation of all pixels in the segmented region to the average HU values of that region as follows.

$$VCSD = \frac{SD}{\mu} \quad (2)$$

, where VCS D means variation coefficient of stone density, SD and μ are the standard deviation and average HU of all pixels in the segmented region.

F. Internal Structure of the Stone

Stone composition is impossible to be completely depend on stone SD or average HU. It can differ even if their SD or average HU are similar values. Therefore, showing the internal structure of stone is a vital role to show stone homogeneity or heterogeneity. In this study, stone structure was described by evaluating the HU values of each pixel of the stone region as following algorithm.

Step 1. Set $HU = (x_1, x_2, x_3, \dots, x_i)$, x_i is represented the HU values of each pixel in the specified region.

```

Step 2. For i=1 to i,
    if (  $x_i > 3000$  )
        out =8;
    else if (  $x_i > 2500 \ \&\& \ HU \leq 3000$  )
        out =7;
    else if (  $x_i > 2000 \ \&\& \ HU \leq 2500$  )
        out =6;
    else if (  $x_i > 1500 \ \&\& \ HU \leq 2000$  )
        out =5;
    else if (  $x_i > 1000 \ \&\& \ HU \leq 1500$  )
        out =4;
    else if (  $x_i > 500 \ \&\& \ HU \leq 1000$  )
        out =3;
    else if (  $x_i > 200 \ \&\& \ HU \leq 500$  )
        out =2;
    else
        out =1;
End
End

```

In here, 1,2,3,...,8 is described as the eight different colors to represent each pixel intensity range.

Step 3. Display with each value of pixels with 1,2,3,...,8.

G. 3D Visualization

After CT acquisition DICOM images were used for preprocessing, a series of slices including ROI stone region were outputted as the segmented results. Preprocessing could provide the 3D object without disturbance such stone, bone and stent. These slices were used to reconstruct 3D model by isosurface-matlab-function that can extract isosurface data from 3D volume array [9]. The 3D object model is based on contours acquired from the ROI segments on all slices including the stone. This 3D stone could provide the shape of the stone, number of stone and location of stone. Because of rotation options, the shape of stone is clearly viewed with low disturbance. Figure illustrated the visualized objects which was implemented with rotation options.

IV. RESULTS

The proposed solution was evaluated using the CT dataset comprising of 22 patients diagnosed with urinary calculi. The experiments have been done by using MATLAB 2020a on an Intel Core i7.

A. Manual 2D Measurement

Stones are irregular structures. So, it is typically assessed by measuring the stone parameters such as area, standard deviation and average HU. In manual measurement, a largest slice is selected manually from all slices including the stone. Next, stone area selection is manually approximated by an ellipsoid and then the system can generate the stone parameters on this area as shown in Figure 3. Stones are irregular structures, such as round, oval, jagged and unsmooth shapes. If stone has smooth boundary, this can be done easily with manual measure and the results are also very similar to 2D auto process. If not, it is impossible to provide the exact results because area selection by ellipsoid is not sufficient to measure the overall stone area. It was depended on the decision of technician and the application they used. Moreover, it may become variability between readers which can give inaccurate information for treatment planning.



Fig. 3. Results of 2D manual measurements.

B. 2D Auto Measurement

The proposed 2D process is automatic and accurate. It can provide the specific CT parameters with a largest slice selection. Figure 4 shows the obtained result for the case introduced in Fig. 3. The proposed 2D process can provide very similar results to the manual process and can be considered as satisfying. Because of fully automatic process including slice selection and stone area selection, it can overcome the limitation of manual process. Without using ellipsoid tool, it can do area selection of any stone structure, smooth or unsmooth boundary. It can set as a definite slice for slice selection because the largest slice is chosen by comparing the stone area of all slices. Moreover, the selected slice is effective and efficient as it can reveal the intensity value of each pixel in slice that are taken to display the internal structure of the stone. Smoother the surface of the stone, the more similar result of 2D processes have. Therefore, it allows the exact results with the

completely automatic ROI recognition and largest slice selection.

```

Command Window
rw : 92
***** Case Hits. Three D *****
Hit Count : 1
i : 51
TwoD Average HU is 1104.5212
TwoD Standard Deviation is 357.7286
TwoD Variation Coefficient is 0.16806
ThreeD Average HU is 977.615
ThreeD Standard Deviation is 370.0374
ThreeD Variation Coefficient is 0.18487
====Finish====
fx >>
    
```

Fig. 4. Results of 2D and 3D auto measurements.

The proposed 2D auto system gives the required CT parameters outputs with the addition of internal structure to predict stone composition.

C. 3D Auto Measurement

The proposed 3D process is too robust as all voxels in all slices including the stone are considered to provide volumetric information for the required parameters. All parameters of 3D process are developed the methods used in 2D auto process. Unlike 2D process, it used all slices including the stone. Exemplary results after CT parameter measuring for auto 2D and 3D processes can be seen in Figure 4. In terms of SD and VCSD, there was no significant difference between the 2D and 3D process although average HU of 3D was lower than that of 2D process. The estimated results of proposed 3D are not perfectly accurate but robust and close enough to be used as CT parameter estimation. It is also completely automatic system that can reduce variability to give better information for treatment planning.

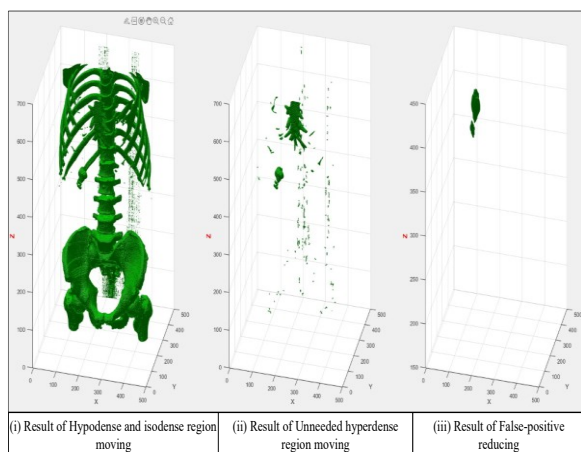


Fig. 5. 3D Visualization output of 3D auto measurements.

Moreover, visualization of 3D image can be provided without any other unwanted region using pre-processing and segmentation as shown in Fig. 5. In visualization result, it is able to provide a clear 3D visual output to analyze the location, number, condition and shape of the stone. As it can rotate in all

direction, it can reduce some unclear visual by overlapping the stone each other.

D. Stone Internal Structure

Showing internal structure of the stone is one of the vital roles to predict fragility of the stone. Stone fragility is also important in some treatments. Homogeneous stones might be less fragile than heterogeneous ones. Therefore, this study is showed the internal structure of the stone to predict that heterogeneous or homogeneous stone. Using the algorithm, the stone composition was shown by defining each pixel with respective colour as shown in Fig. 6.

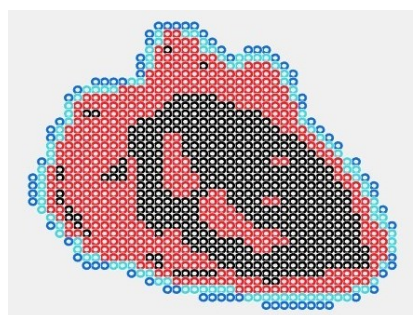


Fig. 6. Internal structure of the stone.

The more SD vale of the stone, the more heterogeneity of the stone composition is in Fig. 7. Showing internal structure in effective and efficient. It can clearly show that the stones having different SD, may have the different structure and heterogeneity. The use of internal structure for determining the heterogeneity of stone before ESWL helps to predict the outcome of the treatment.

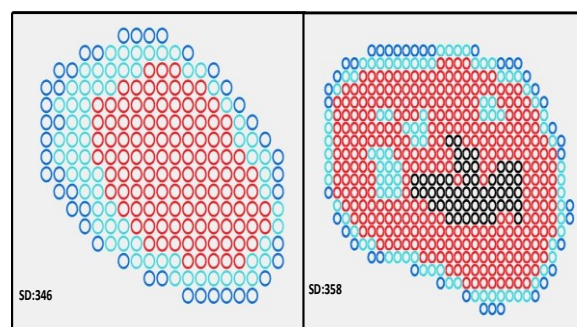


Fig. 7. Showing the heterogeneity of stone with SD.

E. 3D Visualization

3D visualization is one of the fundamental processes in urinary stone diagnostics. Using the acquired 3D images, it is possible to find the structure, size and location of stone, which is the evidence of a specific disease. After the proposed pre-processing was removing all unwanted objects (including bone and stent), it could present 3D output object without disturbance. Due to the 3D reconstructed object, it was possible to analyse the shape of the stone by rotating it in all directions. Figure 8 illustrates an example of 3D visualization result in some directions.

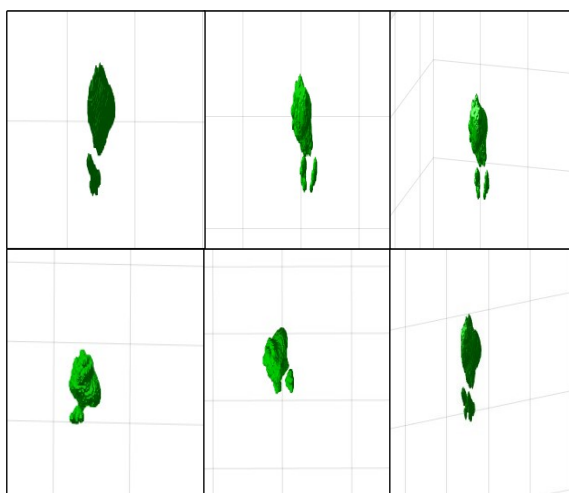


Fig. 8. 3D stone visualization of a patient from some directions.

To evaluate the proposed 3D visualization, RadiAnt DICOM Viewer application was used in this study. According to these experiments in Fig. 9, the proposed scheme can achieve the 3D object more clear and lower disturbance than application used result.

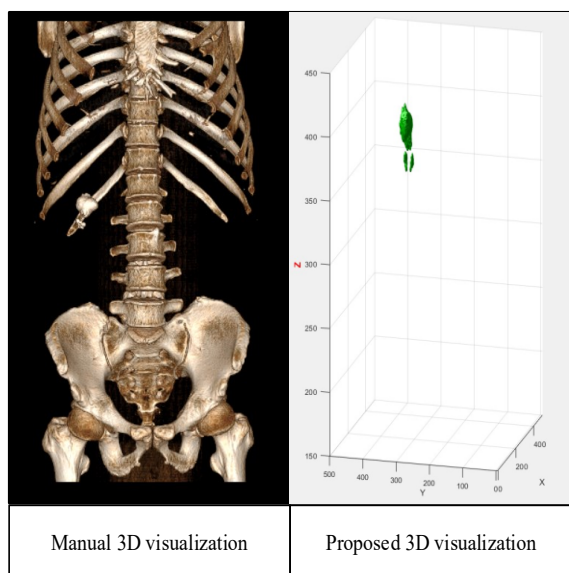


Fig. 9. Results of 3D visualization for manual and 3D process.

V. PERFORMANCE EVALUATION

The results (standard deviation, average Hu and variation coefficient of stone density) of the study among patients clinically diagnosed with manual 2D measurement (2D Manual), auto 2D measurement (2D auto) and auto 3D measurement (3D auto) are compared to evaluate the proposed study as shown in the Table 1. The results computed in Table 1 are used to evaluate the performance of the proposed processes.

The proposed 2D and 3D measurements are qualitatively and quantitatively assessed and compared with manual measurement based on three kinds of criteria as follows:

Average: Firstly, the parameters resulted from the proposed two processes are compared with manual

results by average. It is a fundamental performance measure to calculate the distance between two sets. Average is calculated by adding the values in a set and then dividing by the count of those values.

$$Average = \frac{Total\ Amount}{Number} \tag{3}$$

Correlation: A correlation analysis is applied to identify the relationships between the proposed system and manual.

$$correl(X, Y) = \frac{\Sigma(x-\bar{x})(y-\bar{y})}{\sqrt{\Sigma(x-\bar{x})^2 \Sigma(y-\bar{y})^2}} \tag{4}$$

, where \bar{x} and \bar{y} are the mean average of group 1 and group 2. When 2D auto assumes as group 1, manual is group 2. When 3D auto assumes as group 1, manual is group 2. According to this assumes, correlation between proposed system and manual is calculated. As much as the correlation is closer to 1 and 0, indicates strong and weak correlation between two group, respectively [11].

Accuracy: This criterion measures the accuracy of the proposed system by comparing the system results (predict) and manual results (actual) by using this formula.

$$Accuracy = 1 - (ABS((Predicted/Actual) - 1)) \tag{5}$$

ANalysis of VArance (ANOVA): It is used to determine whether there are any statistically significant differences between the means of two or more independent groups. ANOVA return with a table summarizing the SS (squared deviations), MS (mean square), df (degree of freedom), F value (analysis of variance) and p-value (probability)[12]. Among them, F-statistic and p-value are used in this study.

$$F = \frac{MSB\ (variance\ between\ groups)}{MSW\ (variance\ within\ groups)} \tag{6}$$

p-value means the probability that the observed difference or larger in the means is due to random chance. In this analysis, F value and p-value are vital to decide the similarities or difference within and between groups. If F value is less than F critical, and then p-value is also greater than the alpha level, there is no significantly different within and between the comparison groups.

In all, 22 urinary calculi used to evaluate the proposed 2D and 3D measurements and then the results are compared with 2D Manual measurements as shown in Table I.

In Table II, it is summarized the results of each analysis of the proposed study.

In SD, there was almost the same values in average, sum and variance among the three groups. 2D auto was more strong correlation and accuracy with 2D manual measurements than 3D auto measurements. Moreover, SD with 2D auto was the strongest predictor of accuracy (99%) with 2D Manual.

Table I. CT values by the proposed study and manual record.

| Standard Deviation | | | Average HU | | | Variation Coefficient of Stone Density | | |
|--------------------|---------|---------|------------|---------|---------|--|---------|---------|
| 2D Manual | 2D Auto | 3D Auto | 2D Manual | 2D Auto | 3D Auto | 2D Manual | 2D Auto | 3D Auto |
| 488.11 | 474.76 | 468.64 | 1045.54 | 988.49 | 895.52 | 0.47 | 0.48 | 0.52 |
| 371.29 | 367.10 | 411.98 | 1138.29 | 1108.47 | 977.06 | 0.33 | 0.33 | 0.42 |
| 360.00 | 350.31 | 420.35 | 661.56 | 632.41 | 741.78 | 0.54 | 0.55 | 0.57 |
| 396.60 | 393.16 | 413.89 | 748.80 | 724.84 | 750.00 | 0.53 | 0.54 | 0.55 |
| 390.00 | 392.25 | 431.26 | 1319.00 | 1301.47 | 1203.72 | 0.30 | 0.30 | 0.36 |
| 459.30 | 451.11 | 470.84 | 1033.49 | 1057.34 | 952.89 | 0.44 | 0.43 | 0.49 |
| 451.69 | 453.68 | 448.51 | 1023.80 | 950.83 | 850.83 | 0.44 | 0.48 | 0.53 |
| 397.10 | 391.79 | 334.62 | 741.00 | 744.80 | 625.70 | 0.54 | 0.53 | 0.53 |
| 569.40 | 561.16 | 533.30 | 1151.70 | 1141.85 | 1033.84 | 0.49 | 0.49 | 0.52 |
| 330.00 | 326.25 | 245.67 | 596.03 | 597.35 | 479.04 | 0.55 | 0.55 | 0.51 |
| 444.30 | 446.51 | 434.14 | 960.89 | 1017.47 | 925.89 | 0.46 | 0.44 | 0.47 |
| 330.35 | 327.71 | 363.21 | 958.00 | 921.27 | 817.89 | 0.34 | 0.36 | 0.44 |
| 350.70 | 346.11 | 338.03 | 894.78 | 870.54 | 802.67 | 0.39 | 0.40 | 0.42 |
| 474.48 | 471.35 | 385.25 | 898.78 | 895.08 | 693.19 | 0.53 | 0.53 | 0.56 |
| 508.12 | 499.46 | 497.37 | 1139.77 | 1002.55 | 881.11 | 0.45 | 0.50 | 0.56 |
| 357.57 | 357.73 | 370.04 | 1077.75 | 1104.52 | 977.62 | 0.33 | 0.32 | 0.38 |
| 447.59 | 443.23 | 420.50 | 791.63 | 777.64 | 684.37 | 0.57 | 0.57 | 0.61 |
| 387.10 | 387.10 | 375.03 | 789.58 | 789.58 | 707.84 | 0.49 | 0.49 | 0.53 |
| 413.66 | 415.49 | 415.13 | 913.48 | 903.43 | 816.16 | 0.45 | 0.46 | 0.51 |
| 338.66 | 338.21 | 362.44 | 918.11 | 886.68 | 862.32 | 0.37 | 0.38 | 0.42 |
| 473.90 | 471.57 | 501.12 | 1148.60 | 1162.20 | 1079.85 | 0.41 | 0.41 | 0.46 |
| 528.21 | 528.42 | 466.40 | 998.20 | 899.67 | 782.97 | 0.53 | 0.59 | 0.60 |

Table II. Summarization the results of each analysis of the proposed study.

| Standard Deviation (SD) | | | | | Compare with Manual | | | |
|---|-------|----------|---------|----------|---------------------|-----------------|----------------|--------------|
| Groups | Count | Sum | Average | Variance | Correlation | F (F crit=4.07) | p-value(=0.05) | Accuracy (%) |
| 2D Manual | 22 | 9268.13 | 421.28 | 4604.39 | 1.000 | | | |
| 2D Auto | 22 | 9194.48 | 417.93 | 4472.33 | 0.998 | 0.03 | 0.870 | 99% |
| 3D Auto | 22 | 9107.72 | 413.99 | 4268.58 | 0.815 | 0.13 | 0.718 | 92% |
| Average HU | | | | | Compare with Manual | | | |
| Groups | Count | Sum | Average | Variance | Correlation | F (F crit=4.07) | p-value(=0.05) | Accuracy |
| 2D Manual | 22 | 20948.78 | 952.22 | 32357.53 | 1.000 | | | |
| 2D Auto | 22 | 20478.51 | 930.84 | 31377.67 | 0.972 | 0.16 | 0.693 | 97% |
| 3D Auto | 22 | 18542.25 | 842.83 | 26350.30 | 0.913 | 4.48 | 0.040 | 87% |
| Variation Coefficient of Stone Density (VCSD) | | | | | Compare with Manual | | | |
| Groups | Count | Sum | Average | Variance | Correlation | F (F crit=4.07) | p-value(=0.05) | Accuracy |
| 2D Manual | 22 | 9.96 | 0.45 | 0.007 | 1.000 | | | |
| 2D Auto | 22 | 10.11 | 0.46 | 0.007 | 0.972 | 0.08 | 0.778 | 97% |
| 3D Auto | 22 | 10.97 | 0.50 | 0.004 | 0.899 | 4.14 | 0.048 | 91% |

It can prove that the statistical analysis of each process is no significantly different between each individual and their group mean because of its result, $F(0.03 \text{ and } 0.13) < F \text{ crit}(4.07)$ and $p\text{-value}(0.87 \text{ and } 0.718) > \text{the alpha level}(0.05)$. Therefore, the proposed two measurement systems are reasonable to apply in SD parameter prediction for CT.

The average HU of 2D Manual and 2D Auto was no significantly different, but there was a slightly difference average HU between 2D Manual and 3D Auto. Compare with 3D Auto, 2D auto was more accurate (97%) and correlate (0.972) with 2D Manual. It can predict success because of its statistical analysis results, $F(0.16) < F \text{ crit}(4.07)$ and $p\text{-value}(0.693) > \text{the alpha level}(0.05)$. 3D auto was also useful in good prediction because of its results, $F(4.48) \approx F \text{ crit}(4.07)$ and $p\text{-value}(0.04) \approx \text{the alpha level}(0.05)$. Therefore, 3D auto is also useable as success predictor, likely 2D auto gave the accurate parameter values with Manual.

Based on the summary of VCSD analysis, it can conclude that there is almost the same VCSD average and variance of 2D auto and Manual between each individual and their groups. 3D auto was also no dramatically increased from 0.46 to 0.5 in VCSD average. It was possible as there was a strong correlation between 2D auto and 2D Manual measuring stone parameters. Moreover, it predicted success included $F(0.08) < F \text{ crit}(4.07)$ and $p\text{-value}(0.778) > \text{the alpha level}(0.05)$, with 97% of accuracy and 0.972 correlation. Although it impossible as predict as 2D auto, 3D auto was available as effective predictor with results, $F(4.14) \approx F \text{ crit}(4.07)$, $p\text{-value}(0.048) \approx \text{the alpha level}(0.05)$, 91% accuracy and 0.889 correlation.

Therefore, nearly all parameters of 2D auto were the same with manual because these parameters are evaluated depend on only a slice. It is the best CT parameters prediction in order to get nearly results with Manual. 3D auto was more robust because its parameters are evaluated using all slices including stone. Moreover, its results were also no significant different with Manual. So, the proposed 2D and 3D are very useful to predict CT parameters for urinary calculi.

VI. CONCLUSIONS

CT is the most commonly used imaging method for evaluating a patient who presents and diagnoses urinary stones. It provides a rapid assessment of stone parameters, size, density, heterogeneity, and number of stone. Several investigators have attempted to predict the heterogeneity and density of stone using available preoperative studies. Stones are irregular structures and can have complex geometric shapes. Therefore, manual measuring is impossible to have exact stone parameters and volumetric information because of the limitation to measure depth of the stone.

The proposed study was developed two kinds of auto measurement system to provide technical support in kidney stone detection and diagnosis Its function to pinpoint the CT values (average HU, stone heterogeneity index and variation coefficient of stone density) as these values provide focused investigation for medical specialists.

Compare with manual record, two proposed methods can measure more accurate estimate of stone burden because the whole process was developed by automatically. This gives timely delivery and cost effective of diagnosis for radiologist. Limitation of manual measurement, the largest slice selection and ROI selection chosen by radiologist, may be variation in the process. The proposed methods can be reduced that variability. Reduced variability can give better information for diagnosis and treatment planning. Especially in jagged, staghorn and unsmooth stones, inaccurate segmentation results given by manual may reduce to estimate the precise CT parameter values. Pre-processing methods used in this study could provide better segmentation results than manual. It is very effective and efficient in CT parameter estimation and output visualization.

The 2D auto can derive more precise measurements than average HU, heterogeneity and VCSD in the manual information. Moreover, it provides internal structure of stone to predict stone composition and heterogeneity. This prediction allows the physician in order to use diagnosis and treatment planning. 3D auto could estimate the more robust CT values for any shaped stone compare with 2D manual and auto measurements because of using all aggregate slices of the stone. It saves the processing time to select the largest slice. Moreover, this 3D auto could provide the clear output with 3D visualization that could rotate in any direction. This low disturbance view could be useful to show stone number, shape and location.

In conclusion, our study suggests that stone parameter measured by 2D auto is the best predictor to assist the stone diagnosis process. The routine measurement of 3D auto is probably the most robust and accurate estimate of the overall stone burden, as it takes stone parameters in all direction and slices including the stone. Our results indicate that the proposed 2D and 3D auto measuring are reliable predictors to assert the precise stone heterogeneity and density for urinary stone diagnosis.

The developed program can be installed on any computer. That will allow the physicians to diagnose the urinary stone images outside the hospitals. The program includes automatic 2D and 3D measurements algorithms that allows making the work of physicians less time consuming. This has presented potential usefulness in urinary stone diagnosis and treatment planning; however, it is only a software development tool and the opinion of radiologists and physicians is needed to validate its result.

REFERENCES

- [1] J. Y. Lee, J. H. Kim, D. H. Kang, D. Y. Chung, D. H. Lee and H. Do, "Stone Heterogeneity Index as The Standard Deviation of Hounsfield Units: A Novel Predictor for Shock-Wave Lithotripsy Outcomes in Ureter Calculi," *Sci. Rep.*, vol. 6, no. 23988, pp. 1–7, 2016.
- [2] S. Yamashita, Y. Kohjimoto, Y. Iwahashi, T. Iguchi, S. Nishizawa, K. Kikkawa and I. Hara, "Noncontrast Computed Tomography Parameters for Predicting Shock Wave Lithotripsy Outcome in Upper Urinary Tract Stone Cases," *Biomed Res. Int.*, vol. 2018, no. 9253952, pp. 1-6, 2018.
- [3] H. Singh, D. Gayen, T. K. Mandal and K. Maiti, "The Efficacy of Hounsfield Unit Density of Renal Calculi in Predicting The Success of ESWL," *Sch. Acad. J. Biosci.*, vol. 4, no. 5, pp. 385-389, 2016.
- [4] W. Finch, R. Johnston, N. Shaida, A. Winterbottom and O. Wiseman, "Measuring Stone Volume - Three-dimensional Software Reconstruction or An Ellipsoid Algebra Formula?," *BJU Int.*, vol. 113, no. 4, pp. 610–614, 2014.
- [5] S. Ebrahimi and V. Y. Mariano, "Image Quality Improvement in Kidney Stone Detection on Computed Tomography Images," *J. Image Graph.*, vol. 3, no. 1, pp. 40–46, 2015.
- [6] R. E. Jacob and J. P. Carson, "Automated Measurement of Heterogeneity in CT Images of Healthy and Diseased Rat Lungs Using Variogram Analysis of An Octree Decomposition," *Jacob Carson BMC Med. Imaging*, vol. 14, no. 1, pp. 1–11, 2014.
- [7] C. Oktay, M. Çoraplı and A. Tutuş, "The Usefulness of The Hounsfield Unit And Stone Heterogeneity Variation in Predicting The Shockwave Lithotripsy Outcome," *Diagnostic Interv. Radiol.*, vol. 28, no. 3, pp. 187–192, 2022.
- [8] K. Krechetova, A. Glaz and A. Platkajis, "3D Medical Image Visualization and Volume Estimation of Pathology Zones," *IFMBE Proc.*, vol. 20, pp. 532–535, 2008.
- [9] N. Thein, T. B. Adjı, K. Hamamoto, and H. A. Nugroho, "Automated false positive reduction and feature extraction of kidney stone object in 3D CT images," *Int. J. Intell. Eng. Syst.*, vol. 12, no. 2, pp. 62–73, 2019, doi: 10.22266/IJIES2019.0430.07.
- [10] N. Iqbal, A. Hasan, A. Nazar, S. Iqbal, M. H. Hassan and B. S. Gill, "Role of Stone Heterogeneity Index in Determining Success of Shock Wave Lithotripsy in Urinary Calculi," *J. Clin. Transl. Res.*, vol. 7, no. 2, pp. 241–247, 2021.
- [11] N. Fenton and M. Neil, "Correlation Coefficient and P-Values: What They Are and Why You Need To Be Very Wary of Them," *Risk Assess. Decis. Anal. with Bayesian Networks*, 2012. [Online]. Available: http://www.eecs.qmul.ac.uk/~norman/blog_articles/p_values.pdf.
- [12] H. Y. Kim, "Analysis of Variance (ANOVA) Comparing Means of More Than Two Groups," *Restor. Dent. Endod.*, vol. 39, no. 1, pp. 74-77, 2014.